

Infrared Thermographic Rapid Analysis of Forced Flow Transition via the Hama Strip

C. Purser¹, P. Marzocca¹, M. Marino¹ and D.A. Pook¹

¹School of Engineering
 RMIT University, Bundoora, Victoria, 3083 AUSTRALIA

Abstract

This study investigates the use of Infrared Thermography (IRT) for assessing forced flow transition using a Hama strip (*trip*) on an internally heated wing section. Rapid identification of boundary layer state, either laminar or turbulent, is of significant interest when determining hydrodynamic loads of a Reynolds scaled model. IRT is a non-intrusive method for quantitative boundary layer analysis with the capability for large surface visualisation.

Testing was conducted on a scale model of the generic SSK-class BB2 submarine sail. Configurations ranged through chord Reynolds numbers (Re) of 5×10^5 and 1.3×10^6 ; trip heights of 0.245 mm and 1.15 mm; and trip locations from 15 to 35% of the chord. An infrared camera was used to record still images of the surface temperature. The temperature from the leading edge is shown to grow at the expected $\Delta T \propto x^{0.5}$; which is characteristic for laminar flow. This verifies that useful quantitative information can be extracted from the IRT data. Scaling of the laminar region between Reynolds numbers shows the experimental Nusselt number (Nu) to collapse with a $Re^{-0.3}$ factor, while simulations collapse with $Re^{-0.5}$; it is suspected this discrepancy is due to thermal losses in the model. Transition location data has been compared against existing flat plate tests and found similar dependence on the ratio between trip height and local displacement thickness; considerations were made to geometrical differences. Trip configurations were assessed for effectiveness in transitioning the flow. Finally, empirical formulae were derived as criterion to size a trip for a required transition point.

Introduction

An infrared technique to visualise the boundary layer state was used for assessment of boundary layer tripping effectiveness. Investigation of boundary layer laminar to turbulent transition is both a fundamental fluid mechanics study and an issue for Reynolds scaled experiments. The location of transition can significantly affect the flow and the performance of an aerodynamic body. For example, at low Reynolds numbers (ratio of inertial forces to viscous forces in a fluid) ensuring transition occurs before the location where laminar flow would separate is of paramount importance for the stall angle of attack of an aerofoil. Successful tripping of submarine appendages is difficult due to the relatively low Reynolds numbers. Varying the incidence angle further complicates the design and assessment of appropriate boundary layer trips; e.g. a trip sized for straight-ahead flow conditions may be under-sized and no longer trip on the leeward side. Defence Science and Technology (DTS) Group has conducted research into the tripping of the BB2 submarine hull, this study aims to define testing methodology and tripping criteria for the sail of the submarine.

The salient flow features within a boundary layer include: Laminar regions, turbulent regions and the associated transition; Tollmien-Schlichting (TS) and Cross-Flow (CF) instabilities; and turbulent flow structures [12]. Work done by Petzold and Radespiel [8] has identified thermographic patterns due to CF instabilities on a sickle-shaped wing section segmented into thirds with increasing sweep angle. The wing was manufactured with a carbon fibre electrical heating element and insulation layers to provide heat uniformity at the surface. Crawford et al. [1,2] compared forced

convective heating and cooling on an unswept wing section where transition is primarily due to the development of TS instabilities. Heat was dispersed across the wing via a thermally conductive aluminium layer backed by electrically heated nichrome wire. Studies have also successfully undertaken in-flight testing with IRT as the primary measurement technique for qualitative analysis of boundary layer phenomena [2,4]. IRT image post-processing further broadens potential for applications in the qualitative and quantitative analysis of the boundary layer states [2,10,11].

Extensive research into the forced boundary layer transition using a cylindrical trip wire has been documented (refer to [12] pg. 470 for further references) and collated into a single graph shown in Figure 1. Here the critical Reynolds number (where $Re_{crit} = U\delta_{1,crit}/\nu$ given free-stream velocity U , the displacement thickness at the transition point $\delta_{1,crit}$ assuming untripped laminar flow, and the kinematic viscosity ν) is shown to be dependent upon the ratio between the trip height k and the displacement thickness at the trip location δ_{1k} . A trendline has been generated for the data points, which has some interesting characteristics:

- 1) The main body of the curve follows quite closely to the curve $Uk/\nu = 900$, which is the representation of an ideal relationship where the location of transition x_{crit} and of the trip x_k are equal (hence transition occurs at the trip location and displacement thicknesses are equal). This is described by equation (1):

$$\frac{U\delta_{1,crit}}{\nu} \propto \left(\frac{k}{\delta_{1k}}\right)^{-1} \Rightarrow \frac{Uk}{\nu} = \text{constant} \quad (1)$$

- 2) At $k/\delta_{1k} < 0.3$ the curve diverges to display natural transition at $k/\delta_{1k} = 0$. The consensus is that trip heights below 30% of the local displacement thickness negligibly effect the transition location.

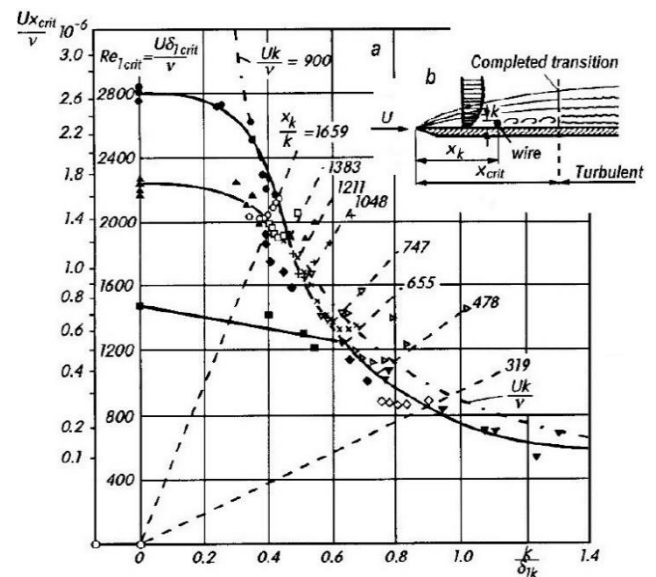


Figure 1. Effect of cylindrical wire tripping device on transition location.

It should be noted that determining the location of 'completed' transition is somewhat arbitrary as transition is not an instantaneous process but rather the breakdown of built up instabilities [5].

Methodology and Instrumentation

Wind Tunnel

Testing was conducted in a closed-return wind tunnel with an octagonal testing section measuring 1370 mm wide, 1080 mm high and 2000 mm long. The tunnel is powered by a 380 kW DC motor driving a fan that provides a maximum windspeed of 42 m/s. With a 4:1 contraction ratio the longitudinal free-stream turbulence intensity in the testing section was measured to be approximately 0.5% [9]. This was a scale model of the low speed wind tunnel (LSWT) at DST Group. A pitot tube mounted 150 mm from the wall of the testing section determined the wind speed. A temperature probe actively adjusted wind speeds to maintain a constant Reynolds number as the ambient temperature changed between tests.

Testing was conducted between chord-based Reynolds numbers of 5×10^5 and 1.3×10^6 , needing a free-stream wind speed range of approximately 8 to 23 m/s; uncertainties at 95% confidence at each of these wind speeds are ± 0.12 and ± 0.25 m/s respectively.

Test Articles and Configuration

Sail: The sail geometry is a scale model of the generic SSK-class BB2 submarine, with an NACA0021 aerofoil with a chord of 865 mm and a span of 400 mm. The sail model was manufactured using a foam core and multiple structural and functional layers shown in Figure 2. Glass Fibre Reinforced Polymer (GFRP) was used to provide structural rigidity and maintain the outer geometry of the aerofoil. An electrically wired layer of carbon fibre acted as a heating element and a thin layer of Depron foam was used to evenly disperse heat to the surface. Car body filler was used to smooth and fill any small surface defects. Finally, a layer of Krylon Ultra Flat Black spray paint provided the high surface emissivity and low reflectivity recommended for IRT testing. This was based off the manufacturing process adopted by Petzold & Radespiel [8], with some alterations due to material test results.

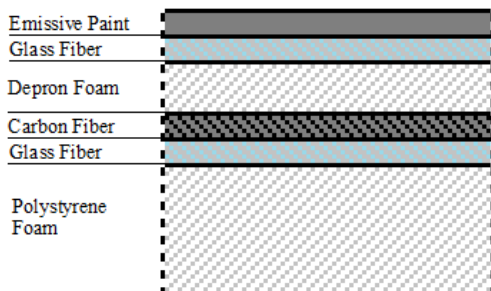


Figure 2. Layer composition of the internally heated sail model.

The outer GFRP layer with body filler smoothing and IR paint has a resulting mean surface roughness (ϵ/c) in the order of $O(10^{-4})$. A rounded cap was manufactured and mounted at the end of the sail. Internal electrical wiring was fed through a hole in the bottom of the ground plane to a 40A DC power supply.

Ground Plane: The sail was mounted on a raised ground plane to minimise the effects of the growing boundary layer on primary flow characteristics of the sail. A secondary effect of the elevated sail was the benefit of a better viewing angle for the IR camera to avoid parallax errors. This ground plane was a medium-density fibreboard (MDF) panel spanning the width of the testing section and mounted along its edges, it was also braced in the centre to minimise vibration.

Hama Strip: The device used to force the flow transition is a Hama strip; a constant thickness strip with a regular saw-tooth pattern that protrudes from the surface to a certain height (k). The Hama strip was used to remain consistent with the BB2 hull tripping tests run by DST Group. Each tooth of the pattern was an isosceles

triangle with base and height of 5 mm, there was a 4 mm band at the base of the teeth that connected them together, shown in Figure 3. The trip was made from layered electrical tape; enabling the trip height to be varied as layers were peeled off, without introducing manufacturing defects between trips. Trip heights were measured before and after tests using a Vernier calliper at multiple points along the trip; the mean was used for calculations. When attached to the sail surface, the troughs of the Hama strip were aligned with the desired chord position. Table 1 details the tested trip heights.

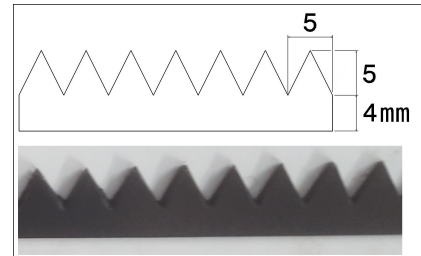


Figure 3. Hama strip tripping device

Trip No.	Layers	Height (mm)
2	2	0.245
3	3	0.372
4	4	0.507
6	6	0.754
9	9	1.15

Table 1. Trip heights used in testing.

Data Acquisition and Processing

IRT data was acquired for surface temperature measurements via a COX CG-640 long wave infrared (LWIR) camera, with a video resolution of 640×480 pixels and 30Hz video sampling. The spectral range of the camera is 8-14 μm . Surface temperatures have an accuracy of $\pm 2\%$ of the reading. Video data acquisition was performed in the initial sets to identify a constant and steady transition profile. It was deemed that the experiments provided adequate consistency and repeatability to allow for single shot photo acquisition for temperature measurement.

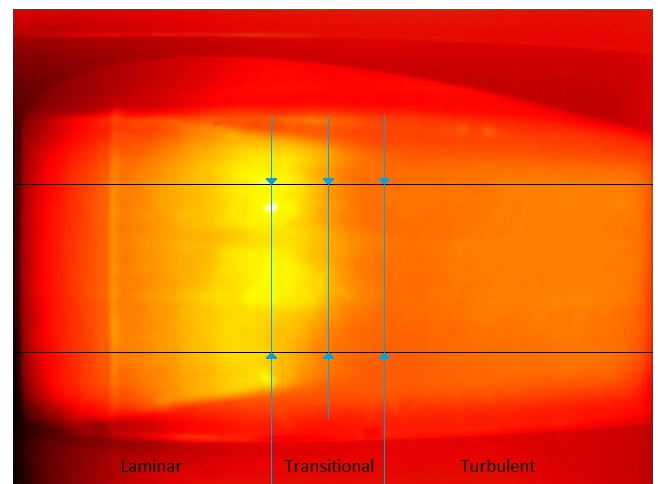


Figure 4. Example IRT image, with trip number 4 at 15% of the chord for $Re = 5 \times 10^5$. Horizontal lines indicate the spanwise invariant data that was averaged for analysis, vertical lines identify flow region boundaries.

The central 50% of the span (shown between the horizontal black lines in Figure 4) was averaged to avoid interferences from the ground plane boundary layer and 3-dimensional flow around the sail cap. This also minimised the error from small surface heating non-uniformities. Three tests were performed for each configuration varying up and down the wind speeds to ascertain repeatability with no identification of hysteresis effects. Data of

the same configuration and wind speed were seen to be concordant, subsequent processing used an averaged run.

With reference to Figure 4, transition was considered ‘complete’ at the location of maximum negative temperature change ($-dT/dx$) (middle vertical line) along the chord (herein to be referred to as the *transition location* or x_{crit}). This transition location was identifiable as approximately halfway between the local maximum (left vertical line) at the end of the laminar region and the local minimum (right vertical line) at the beginning of the turbulent region. This objective location is coincident with the subjective observation of thermal regions on the IRT images.

To assess the ‘effectiveness’ of the trip, a threshold (λ) was used. If the transition occurred at the trip, or within 10% of the chord length behind the trip ($\lambda = 0.1$), the trip was considered effective. If transition occurred further downstream the trip is considered ineffective.

Results and Discussion

Flow Region Identification

Theoretical (Blasius boundary layer) and experimental surface temperature observations on a flat plate show that the chord-wise temperature in laminar and turbulent boundary layers grow to an exponent (b in equation (2)) of 0.5 and 0.2 respectively [7].

$$\Delta T \propto (x - x_0)^b \quad (2)$$

Curve fitting has been applied to the first region of the untripped sail as shown in Figure 5. For each of the three runs, exponents of 0.480, 0.489 and 0.491 were observed. These show consistency between runs and are sufficiently close to the theoretical 0.5 to identify this region as laminar flow. Tripped cases with data of the trip location excluded show congruency.

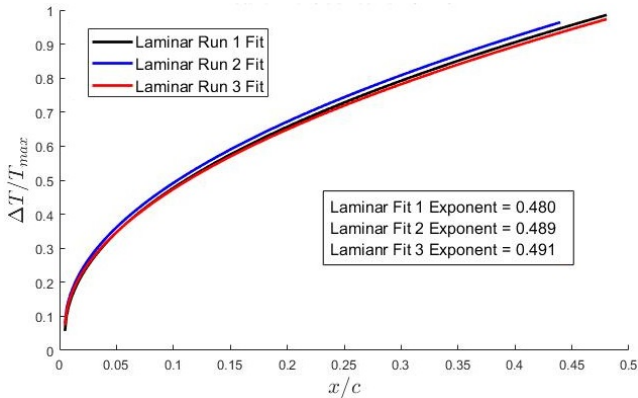


Figure 5. Laminar region of natural transition at $Re = 5 \times 10^5$.

Curve fitting for the turbulent region was unsuccessful due to a lack of distinctive data. The near leading-edge data provides the most characteristic section of the curve; without this, the error for the exponent estimate was too large to be considered accurate.

Figure 6 shows that the Nusselt number (ratio of convective to conductive heat transfer at the wall-fluid boundary) for tests of the same configuration but varying Reynolds number collapse when multiplied by $Re^{-0.3}$. As per the Blasius solution; skin friction, Nusselt number, and shape factor should collapse in the laminar region when multiplied by $Re^{-0.5}$. The discrepancy between these factors is suspected to be due to thermal losses to the foam core of the sail.

Figure 6 is a good example of the transition front moving closer to the trip location as the Reynolds number is increased. The flow state labels correspond to the $Re = 5 \times 10^5$ curve; increasing the Reynolds number moves the transition closer to the trip location.

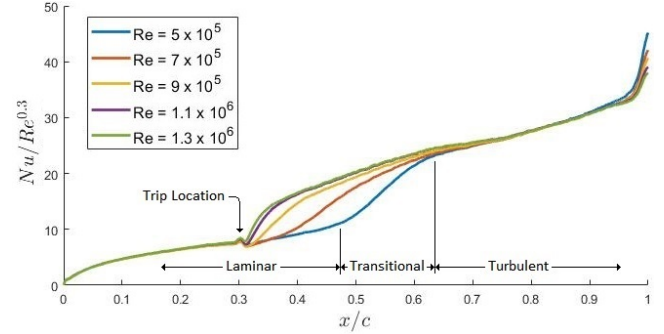


Figure 6. Collapse of tests by $Re^{-0.3}$. Trip height 4, at 30%.

Verifying Forced Transition Tests

Due to lack of equipment to measure the local boundary layer and displacement thickness on the surface: The displacement thickness at the trip location δ_k and the transition location δ_{crit} were estimated using a viscous 2D XFOIL simulation of the NACA0021 aerofoil at the testing Reynolds numbers. This assumes that the sail was manufactured accurately, which was not verified.

Figure 7 represents the Hama strip data using the same axes as in Figure 1. Represented this way there are a few key observations to be made in comparison to Figure 1:

- 1) The bulk of the data lies about the curve where Uk/ν is constant. This constant has changed from 900 in Figure 1 to 730.
- 2) Divergence from the $Uk/\nu = 730$ curve can be seen to occur at $k/\delta_{1k} < 0.3$ until the location of natural transition at $k/\delta_{1k} = 0$.
- 3) Data points that lie further from the $Uk/\nu = 730$ curve can be seen to coalesce around lines of constant x_k/k (represented by dotted grey lines). These are computed using equation (3).

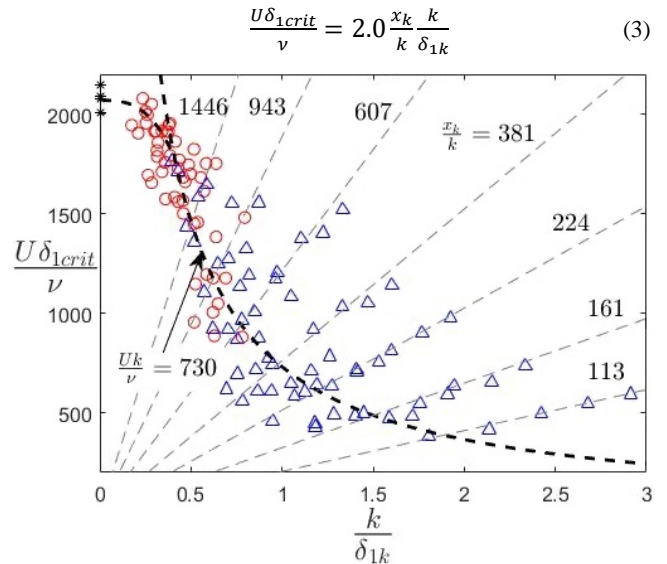


Figure 7. Hama strip data presented with axes as in Figure 1. Triangle and Circle data represent transition before and after the threshold respectively.

When plotted on the same axes as in Figure 1, the IRT data can be seen to follow a very similar trend. The differences in $Uk/\nu = 730$ (rather than 900) and the magnitudes of both the x_k/k constants and location of natural transition can be attributed to the differences in geometry. Where Figure 1 is based upon a flat plate sample with a single roughness cylindrical tripping device, this study uses a thick aerofoil and a Hama strip to trip the flow.

The use of a threshold ($\lambda = 0.1$) is represented by the circular and triangular data points: These indicate whether the flow transitioned within 10% of the chord after the trip location. As there is no clear

division between the circular and triangular data points, the axes in Figure 7 were considered a poor way of representing the data when assessing the effective tripping cases.

Trip Effectiveness and Sizing

Assessing the effectiveness of a trip is rather arbitrary. To improve the representation of trip effectiveness, the data has been plotted in Figure 8. Here the vertical axis represents the distance between the trip and transition as a portion of the chord length. As this is also the definition of threshold λ , it can be represented as a horizontal line. The data as triangles below the threshold represents trips configurations that are considered effective.

The horizontal axis is the product of two ratios: Schlichting [12] and Dryden [3] determined that a $k/\delta_{1k} < 0.3$ provides little to no change in the transition location, and this assessment is supported by the data in Figure 7. It is also important to ensure the trip is not too large, forcing the flow to become 'over-tripped'; the effects of which can persist to 2000 trip heights downstream [6]. A trip height equal to the local displacement thickness has been set as an upper limit $k/\delta_{1k} = 1$. Introducing the ratio between the trip location and transition location helps to normalise onto a single trend line the data that would otherwise diverge.

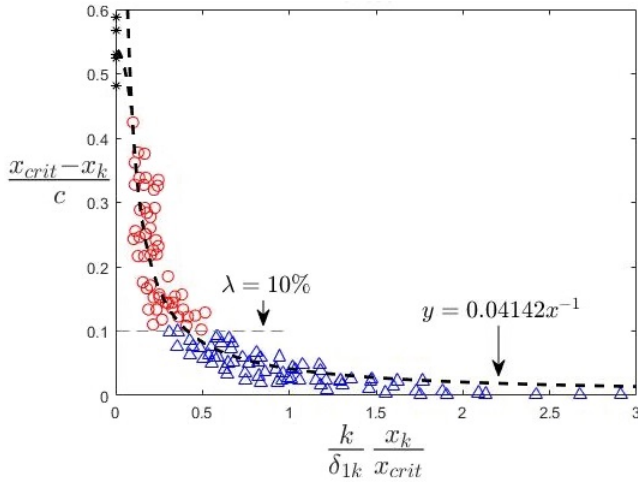


Figure 8. Trip effectiveness compared against a threshold $\lambda = 0.1$, where λ is the distance between the trip and transition points, normalised by chord. Blue and red data represent transition before and after the threshold respectively.

The curve of best fit in Figure 8 is represented as equation (4).

$$\frac{x_{crit}-x_k}{c} = 0.04142 \left(\frac{k}{\delta_{1k}} \times \frac{x_k}{x_{crit}} \right)^{-1} \quad (4)$$

Trip sizing can be determined for a desired transition location x_{crit} , with equation (4) rewritten as equation (5) and the ratio limits shown in equations (6-8):

$$\frac{k}{\delta_{1k}} \times \frac{x_k}{x_{crit}} \times \frac{x_{crit}-x_k}{c} = 0.04142 \quad (5)$$

$$0.3 < \frac{k}{\delta_{1k}} < 1 \quad (6)$$

$$\frac{x_{crit}-x_k}{c} < \lambda \quad (7)$$

$$0 < \frac{x_k}{x_{crit}} < 1 \quad (8)$$

It should be noted that solving these equations is an iterative process as δ_{1k} is dependent upon x_k . If a range of solutions can provide the desired transition location, it is recommended that the solution is optimised for the smallest trip height to minimise downstream wave structures.

Conclusion

Presented are the results of wind tunnel experiments investigating forced flow transition on an internally submarine sail model via infrared thermography. Surface temperature data in the laminar region is shown to grow at the expected $\Delta T \propto x^{0.5}$ until the location of flow transition. Laminar region scaling between Reynolds numbers showed the experimental Nusselt number to collapse with a $Re^{-0.3}$ factor; while simulations collapse with $Re^{-0.5}$. Transition location data has been compared against existing flat plate tests and found similar dependence on the ratio between trip height and local displacement thickness; considerations have been made to geometrical differences. A trip effectiveness threshold of 10% has been adopted to group the trip configurations into effective and ineffective cases. This threshold, along with empirical formulae were used to derive trip sizing criteria for the given geometry and a required transition point.

Acknowledgments

Appreciation goes to the late Dr. Jon Watmuff for starting this project. The authors are grateful for the project motivation and loan of the IR camera by Defence Science and Technology (DST) Group, and the assistance provided by Mr. Paul Muscat on the design and manufacture of the heated wind tunnel model.

References

- [1] Crawford, B.K., Duncan Jr, G.T., West, D.E. & Saric, W. S., Laminar-turbulent boundary layer transition imaging using IR thermography, *Optics and Photonics Journal*, **3**(3), 2013, p. 233.
- [2] Crawford, B.K., Duncan Jr, G.T., West, D.E. & Saric, W.S., Quantitative boundary-layer transition measurements using IR thermography, *52nd Aerospace Sciences Meeting*, 2014, p. 1411.
- [3] Dryden H.L., Review of Published Data on the Effect of Roughness on Transition from Laminar to Turbulent Flow, *Journal of the Aeronautical Sciences*, **20**(7), 1953, 477-482.
- [4] Horstmann, K.H., Quast, A. & Redeker, G., Flight and wind-tunnel investigations on boundary-layer transition, *Journal of Aircraft*, **27**(2), 1990, 146-150.
- [5] Klebanoff, P.S., Cleveland, W.G. & Tidstrom, K.D., On the Evolution of a Turbulent Boundary Layer, *Journal of Fluid Mechanics*, **237**, 1992, 101-187.
- [6] Marusic, I., Chauhan, K.A., Kulandaivelu, V. and Hutchins, N., Evolution of Zero-Pressure-Gradient Boundary Layers from Different Tripping Conditions, *Journal of Fluid Mechanics*, **783**, 2015, 379-411.
- [7] Massoud, M., *Engineering thermofluids*. Berlin Heidelberg: Springer-Verlag, 2005.
- [8] Petzold, R. & Radespiel, R., Transition on a Wing with Spanwise Varying Crossflow Evaluated with Linear Stability Theory, *43rd AIAA Fluid Dynamics Conference*, 2013.
- [9] Ravi, S., The influence of turbulence on a flat plate aerofoil at Reynolds numbers relevant to MAVs, 2011.
- [10] Ricci, R., Montelpare, S. & Silvi, E., Study of Acoustic Disturbances Effect on Laminar Separation Bubble by IR Thermography, *Experimental Thermal and Fluid Sciences*, **31**(4), 2007, 349-359.
- [11] Richter, K. & Schülein, E., Boundary-Layer Transition Measurements on Hovering Helicopter Rotors by Infrared Thermography, *Experiments in fluids*, **55**(7), 2014, 1-13.
- [12] Schlichting, H. & Gersten, K., *Boundary-layer theory*, Springer, 2016.